Developing On-the-fly observations for ALMA

Nemesio RODRIGUEZ FERNANDEZ
Jerome PETY, Frederic GUETH

IRAM

Wide field imaging

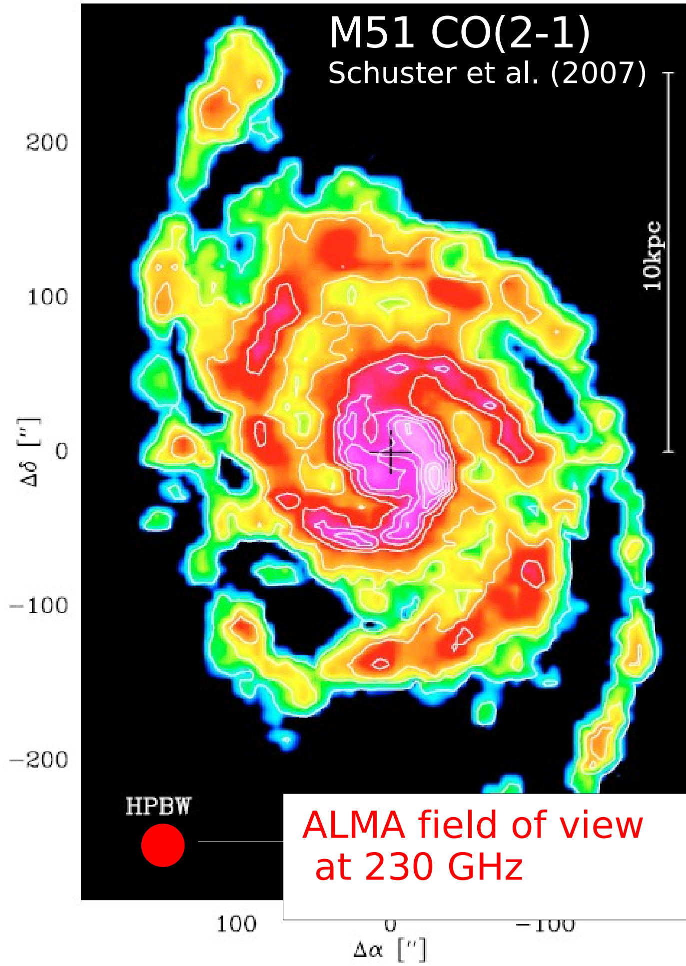

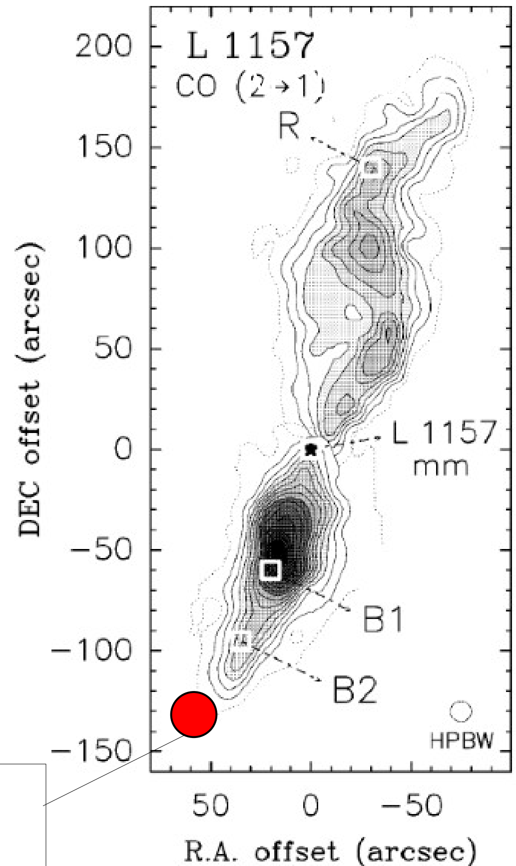

ALMA field of view
at 230 GHz

Mosaics

- Stop-and-go

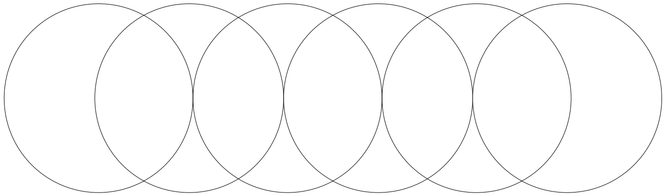

- On-the-fly (OTF)

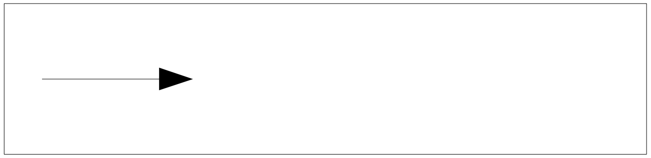

  - Advantages:
    - Faster, time efficient, better quality data
    - Larger fields
    - Open new ways of data editing and processing … although this is non-trivial, never done before

OTF simulator

An OTF simulator simulator

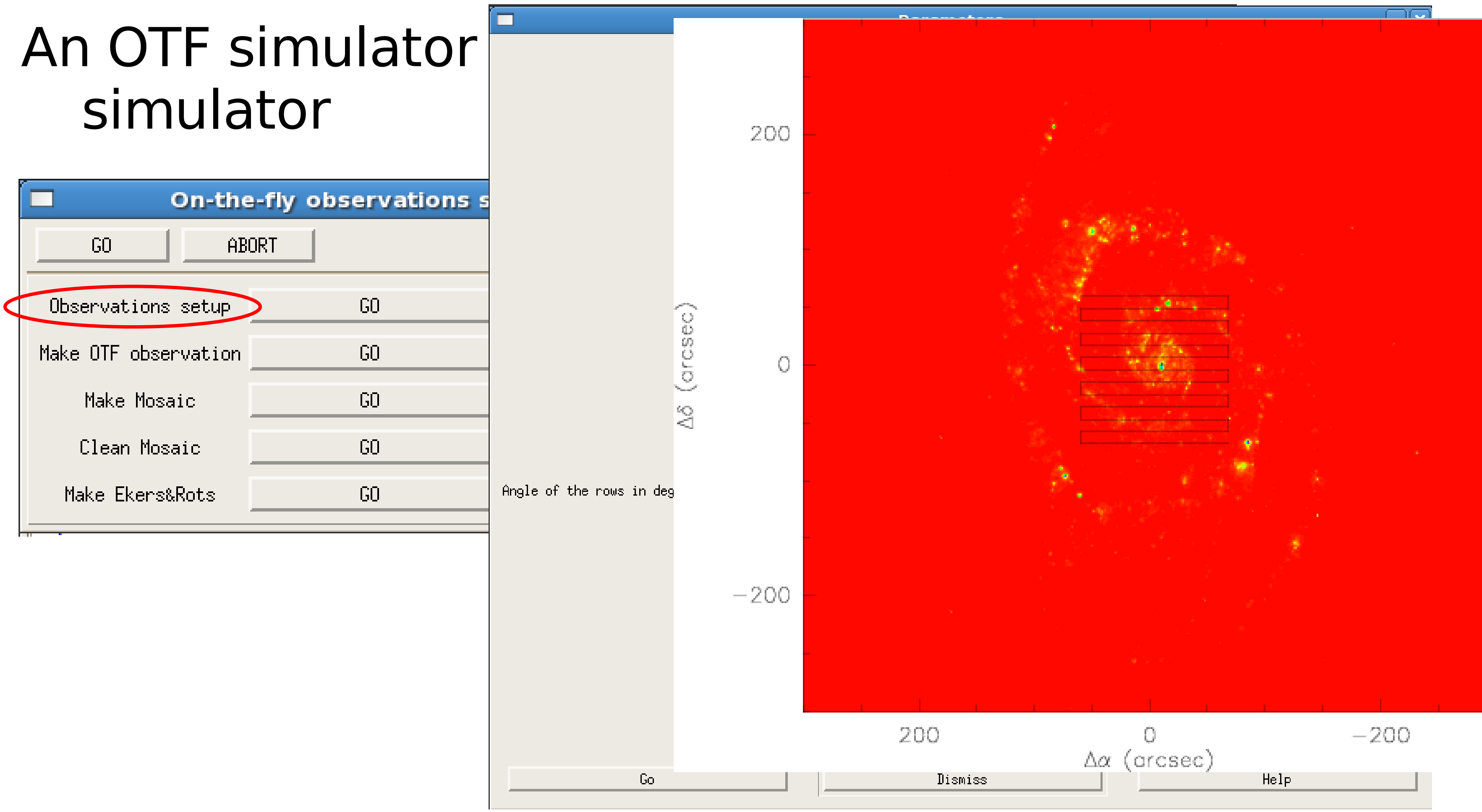

OTF simulator

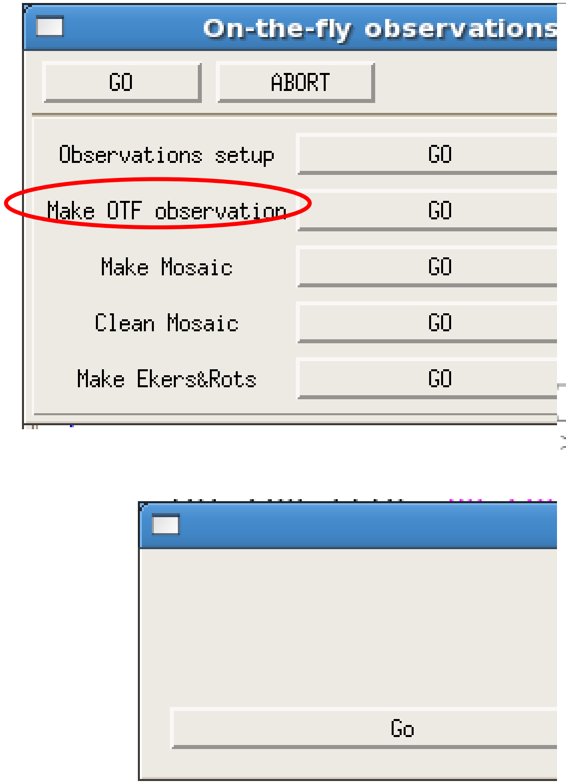

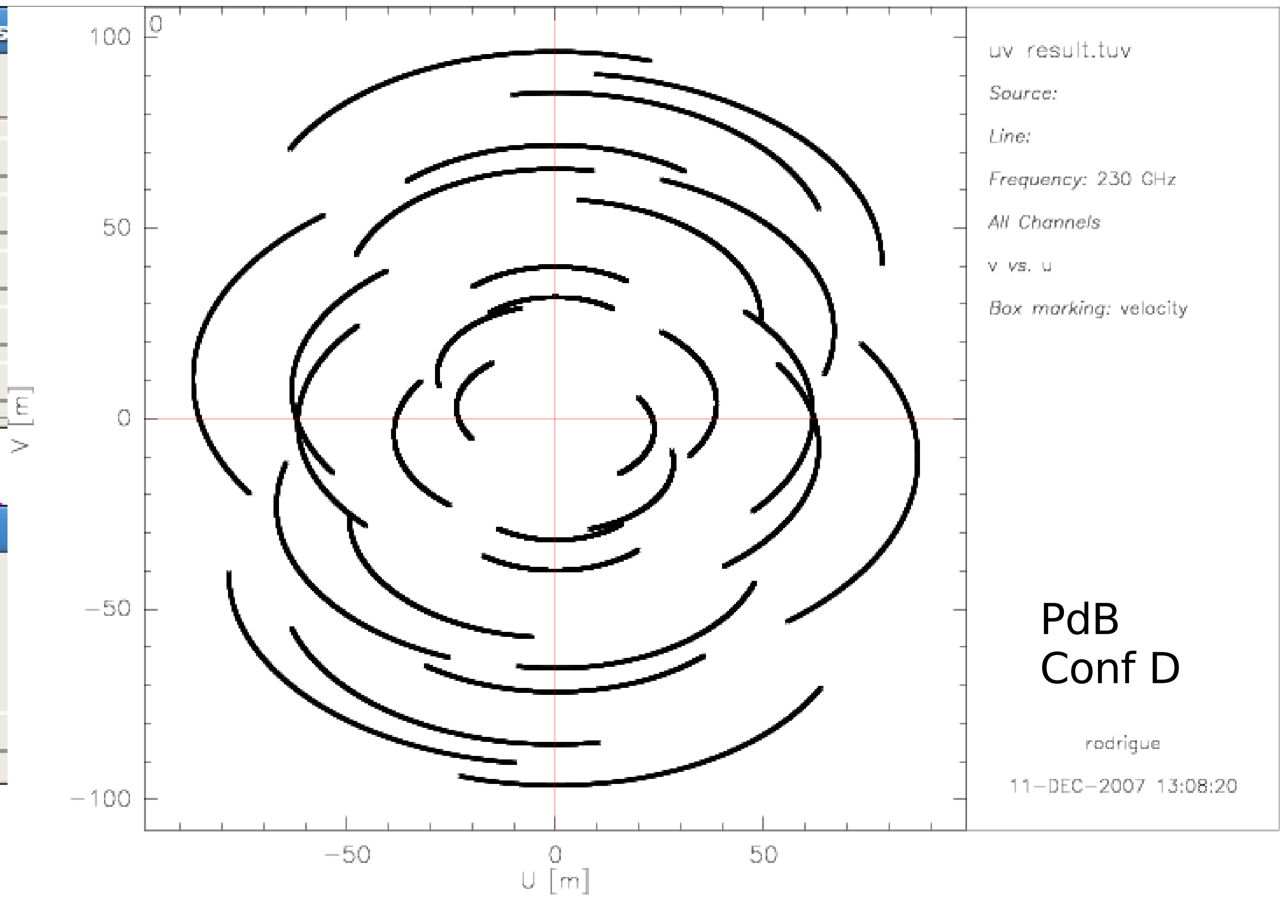

PdB
Conf D

Imaging as a classical mosaic

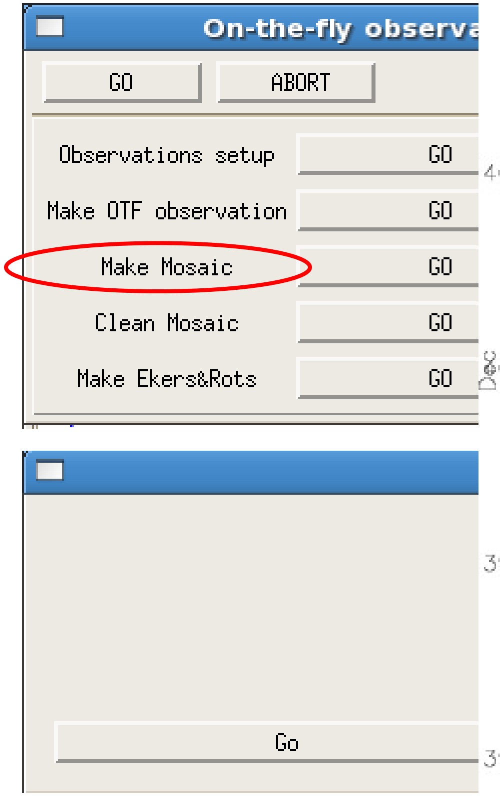

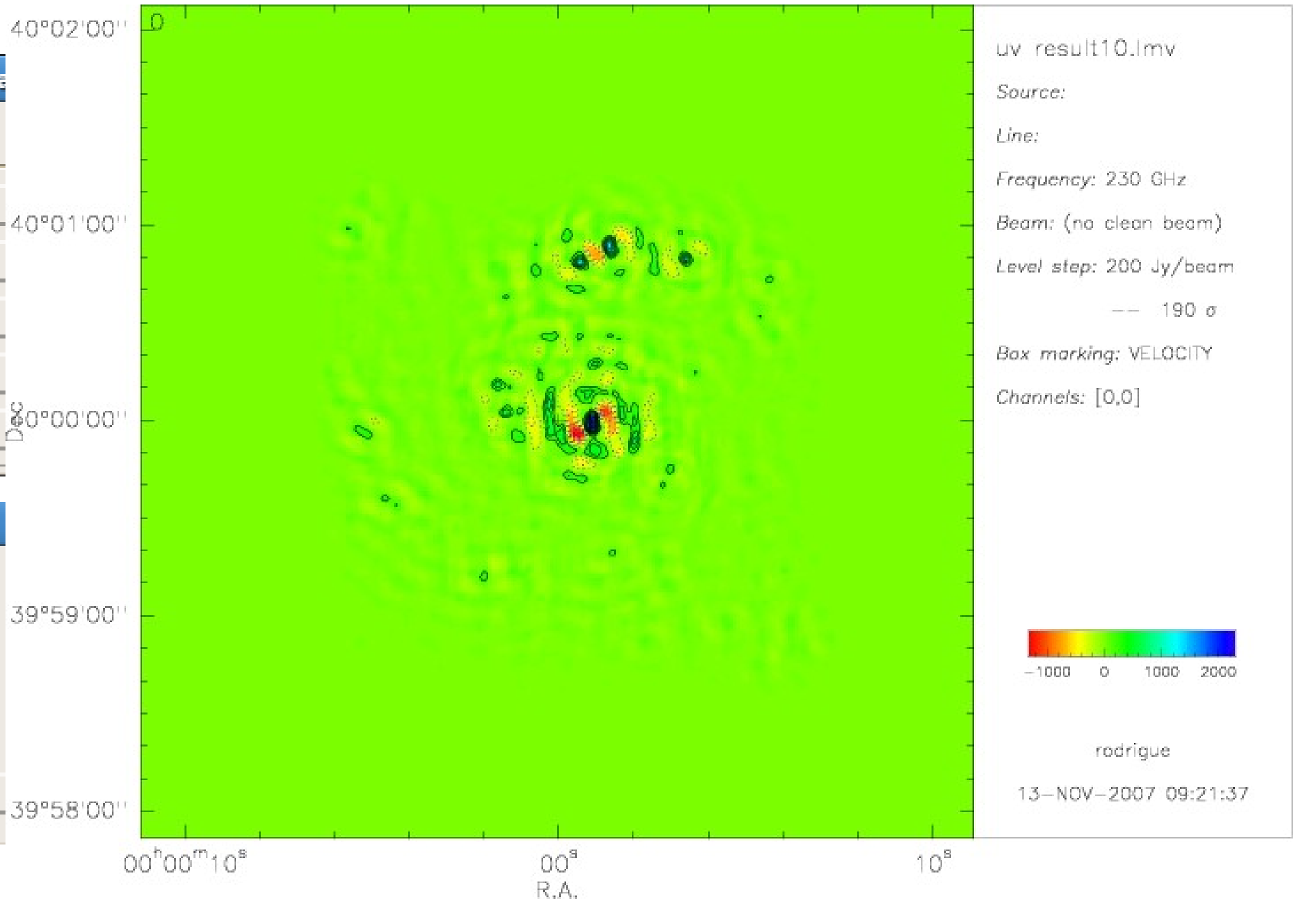

Deconvolution

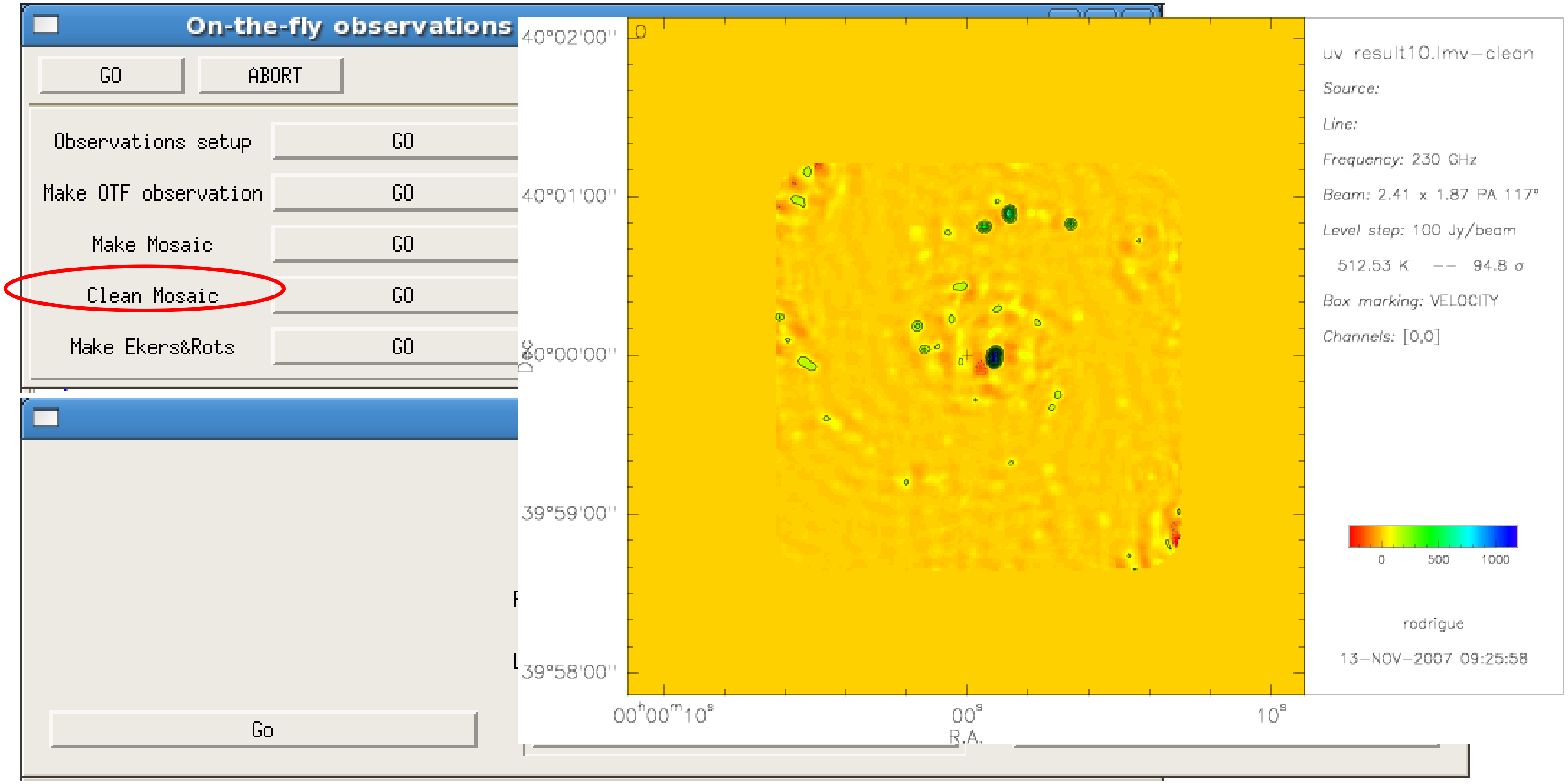

OTF simulator

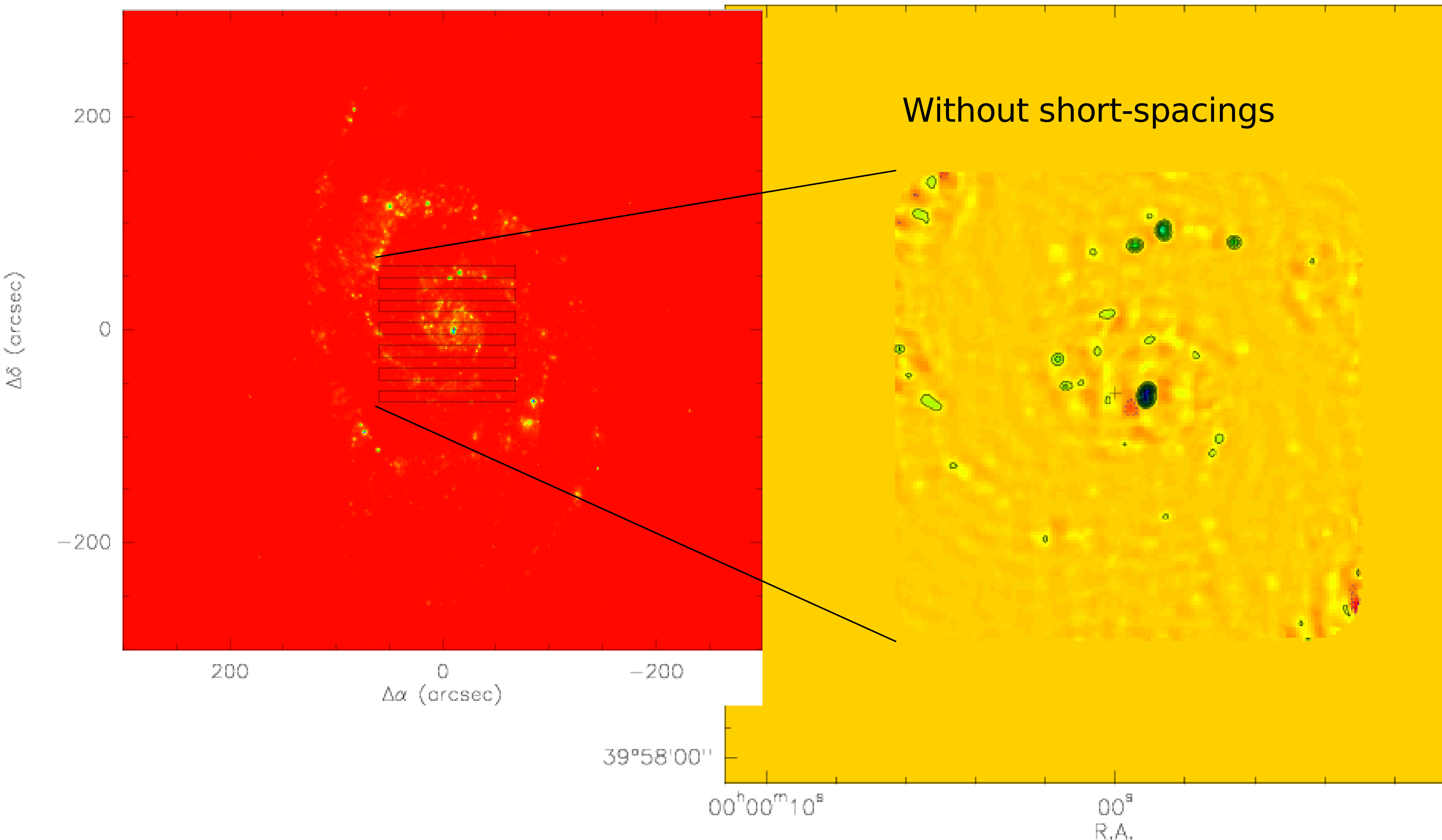

OTF-specific algorithm

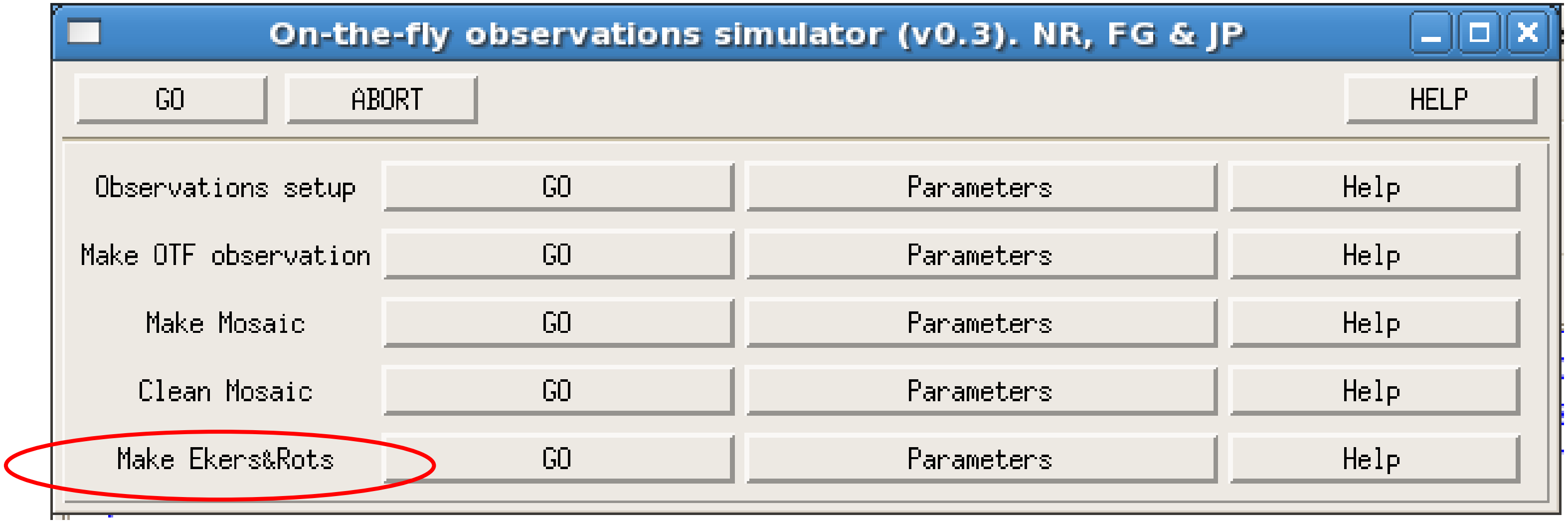

Ekers & Rots (1979)

$$V(u) \equiv \widetilde{B\, I} \equiv \int B(l)\, I(l)\, e^{-i2\pi ul}\, dl$$

$$V(u, l_p) = \int B(l - l_p)\, I(l)\, e^{-i2\pi ul}\, dl$$

$$P(u, u_p) \equiv \int V(u, l_p) e^{-i2\pi u_p l_p}\, dl_p$$; for constant **u**

"super-visibility function"

$$\tilde{I}(u + u_p) = P_u(u_p) / \tilde{B}(u_p)$$ $|u_p| < D/\lambda$ (where $\tilde{B}(u_p) \neq 0$)

Direct measurement of the *true* visibility of the source in the surroundings of the point **u**

ER79: intuitive idea

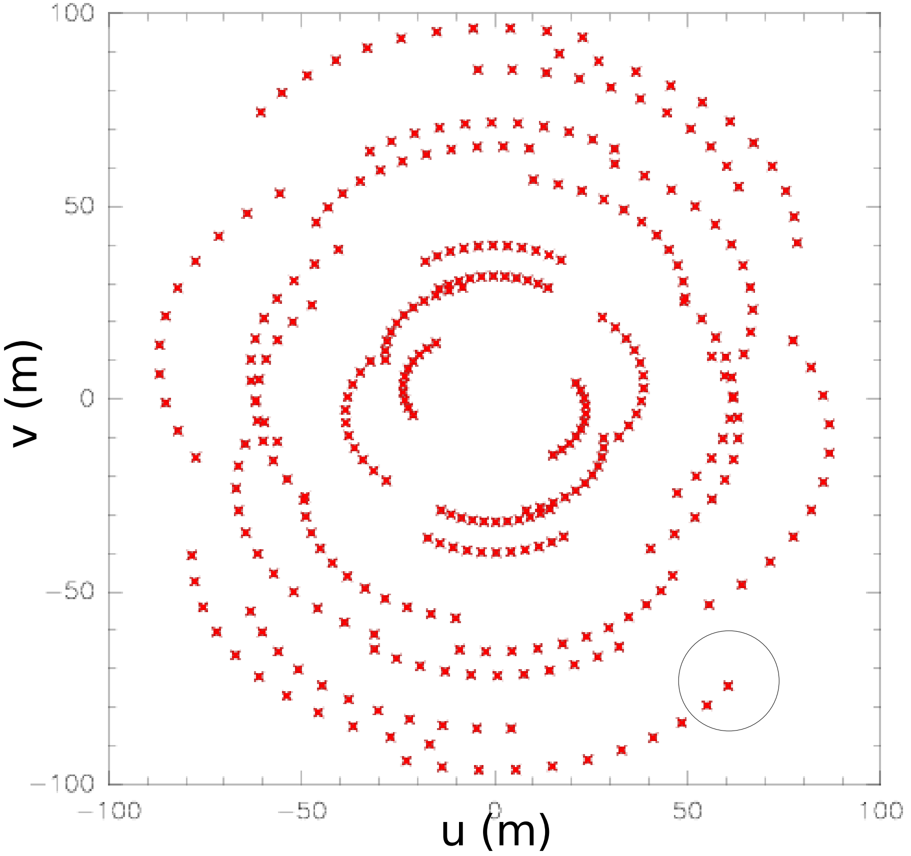

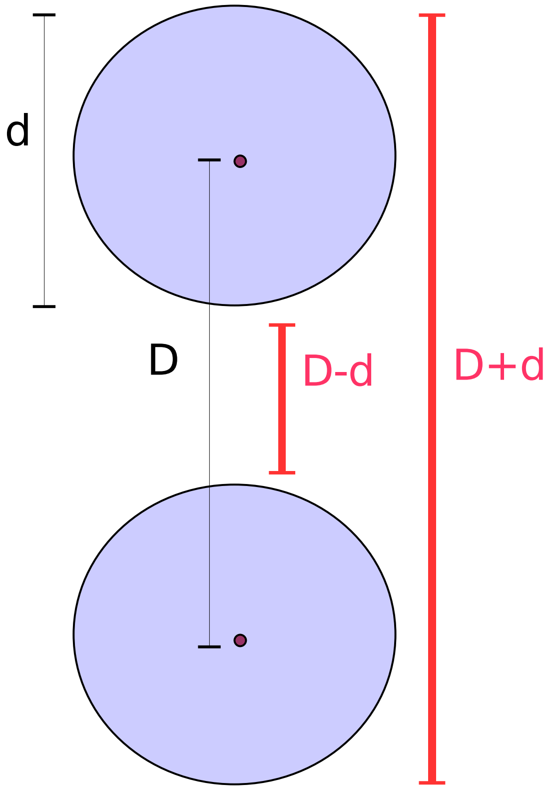

ER79: intuitive idea

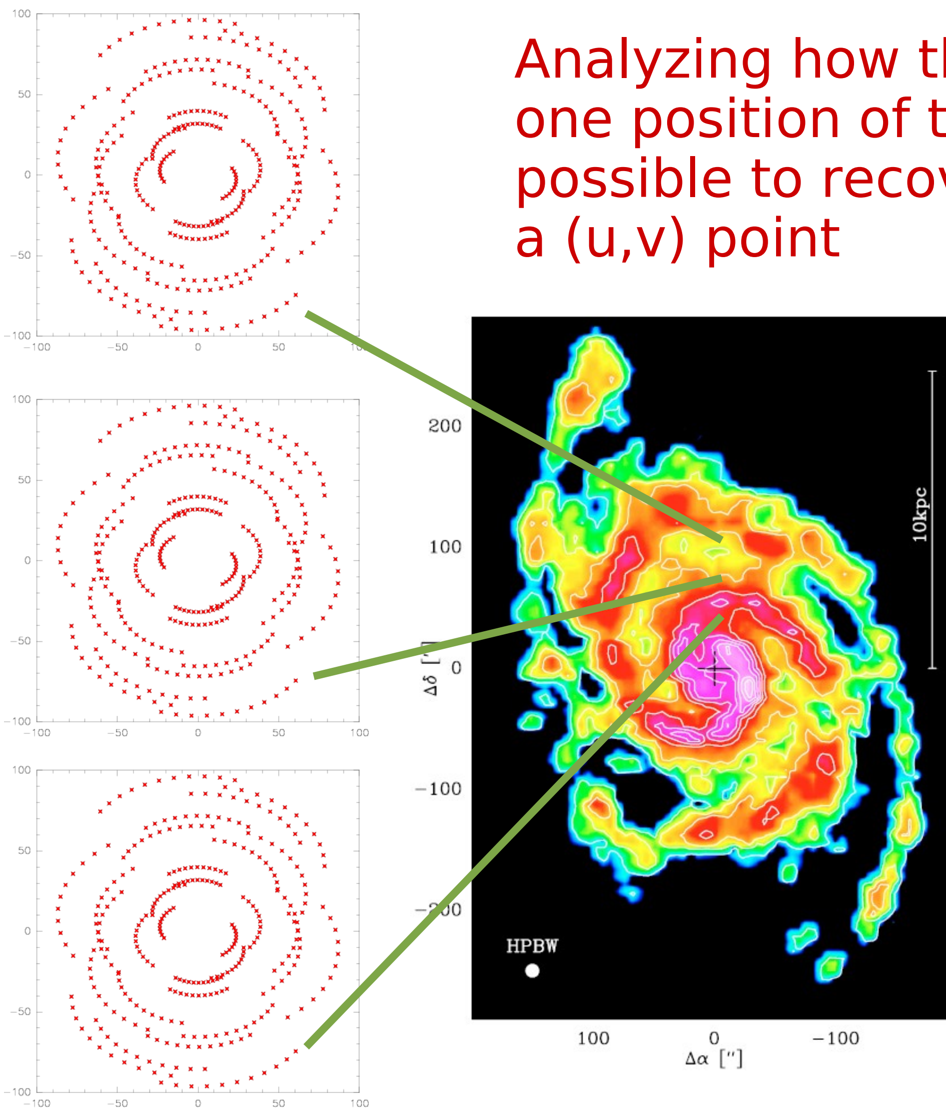

Analyzing how the visibilities change from one position of the source to another, it is possible to recover the information around a (u,v) point

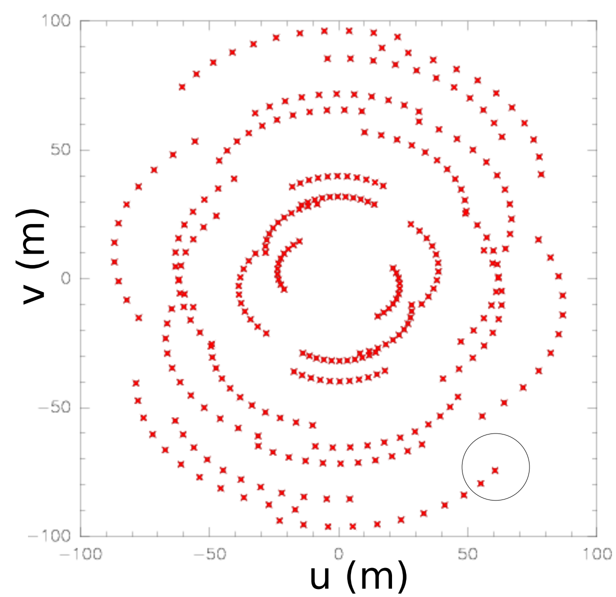

From N_{fields} uv planes to a global "wide-field" uv-plane

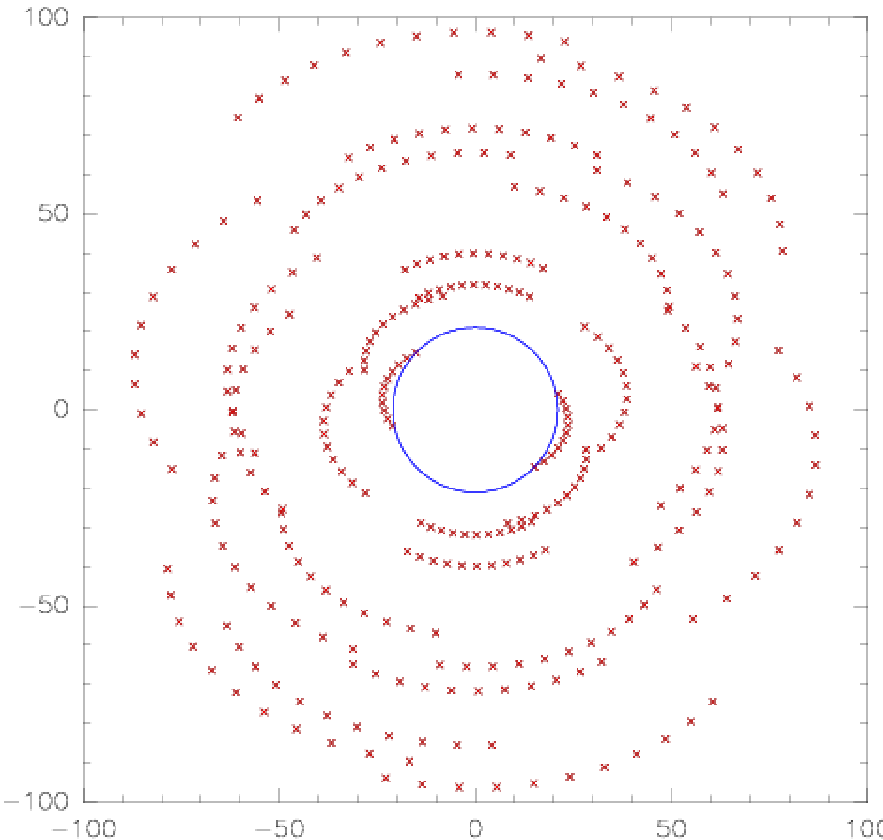

N_{fields} *uv*-planes with "averaged" visibilities

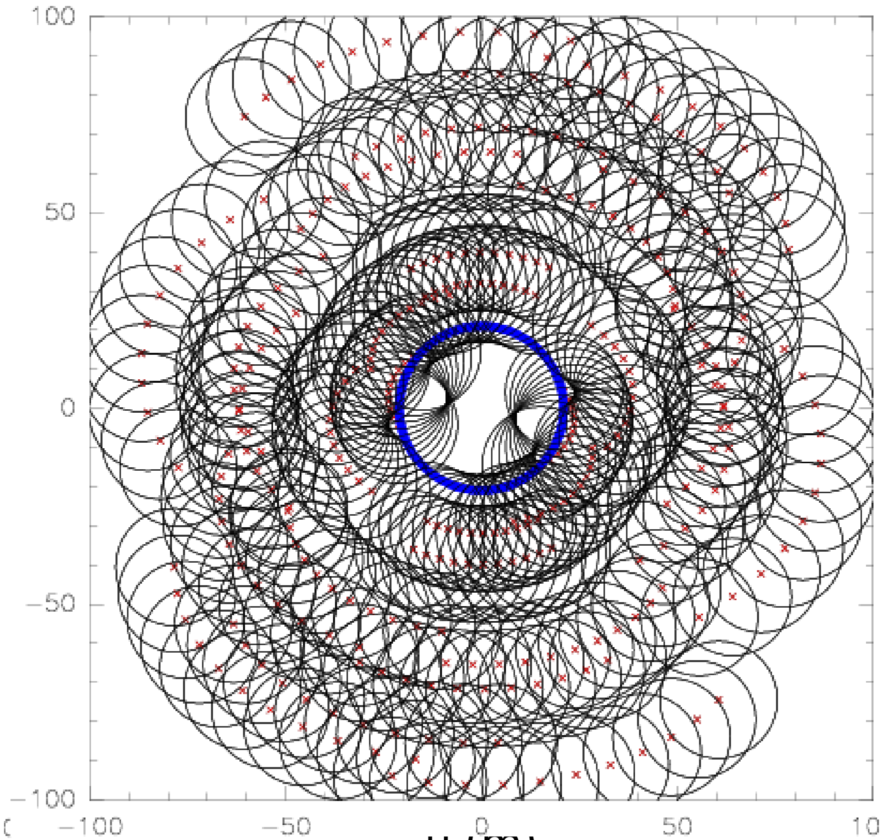

1 uv-plane for the whole mosaic

How to develop an ER79-based algorithm?

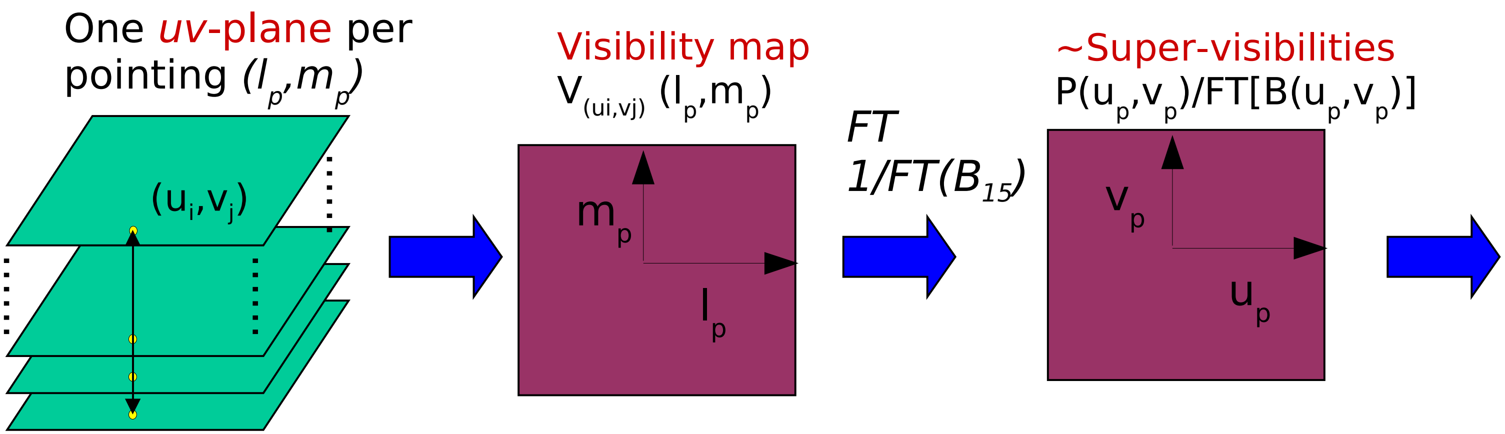

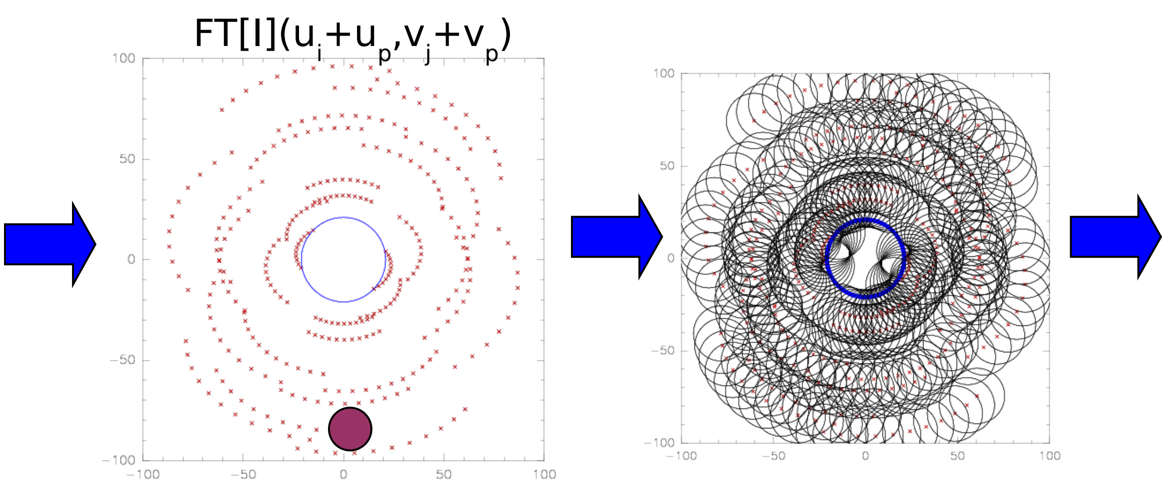

- Weight estimation
- Weighted linear combination of the functions

$$\tilde{I}(u+u_p) = P_u(u_p)/\tilde{B}(u_p)$$

to get the global uv-plane

- Global imaging and deconvolution

How to develop an ER79-based algorithm?

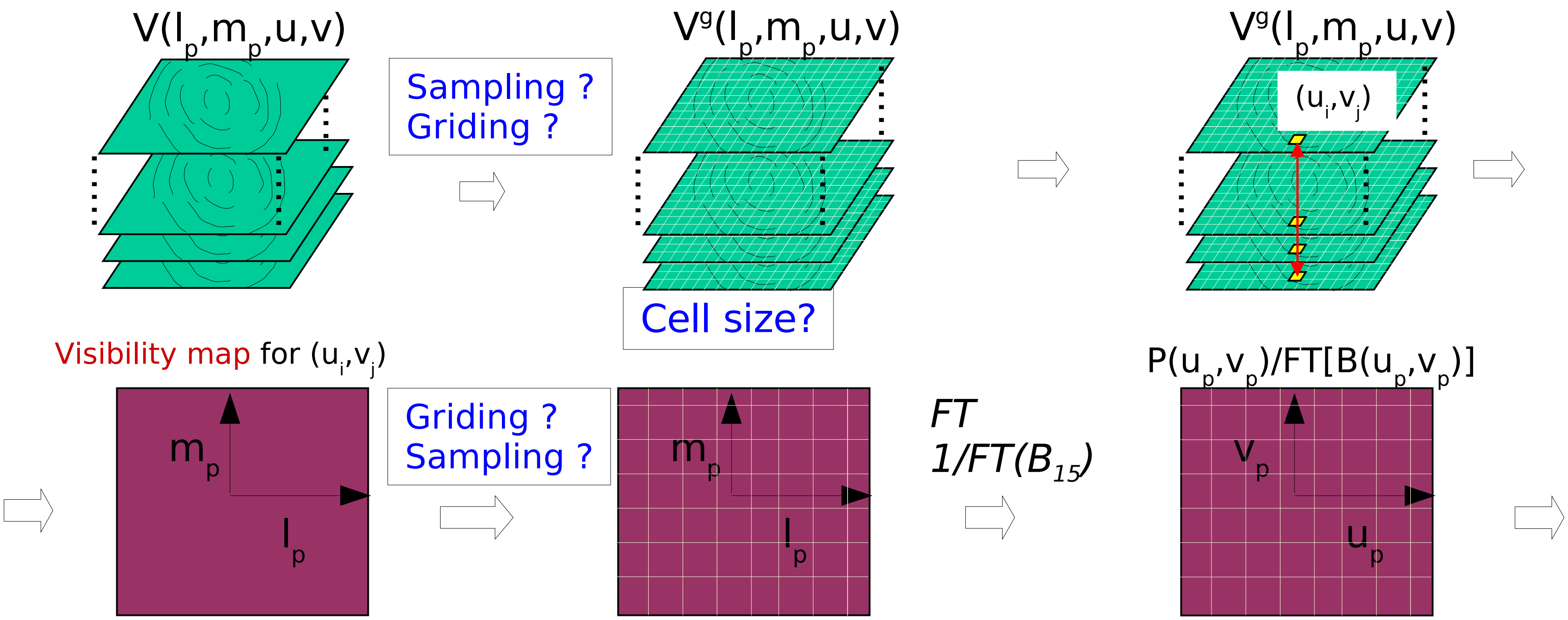

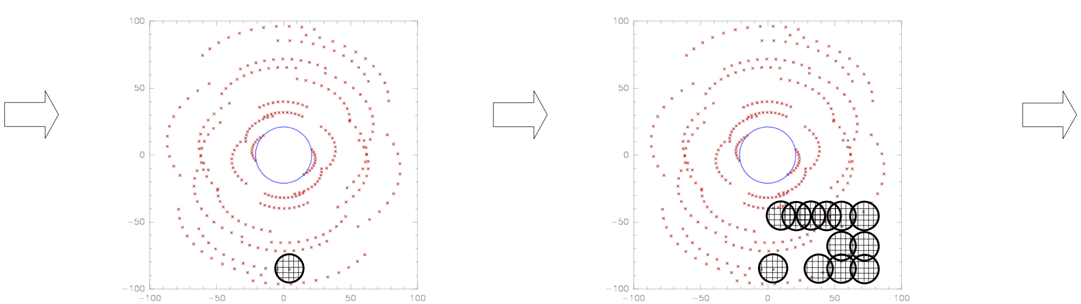

- Weight estimation?
- Weigthed linear combination of the functions

$$\tilde{I}(u+u_p) = P_u(u_p)/\tilde{B}(u_p)$$

to get the global uv-plane

- Global imaging and deconvolution

Griding and sampling in 4D (l_p,m_p,u,v)

$$V^g(l_p,m_p,u,v) \equiv K(l_p,m_p,u,v) * [V(l_p,m_p,u,v) \cdot S(l_p,m_p,u,v)]$$

$$S^g(l_p,m_p,u,v) \equiv K(l_p,m_p,u,v) * S(l_p,m_p,u,v)$$

$$P^g(u_p,v_p,u,v) \equiv FT_{l_p m_p}[V^g(l_p,m_p,u,v)] = \tilde{V}^g(u_p,v_p,u,v)$$

$$\frac{\tilde{V}^g(u_p,v_p,u,v)}{\tilde{K}(u_p,v_p,u,v)} = \frac{\tilde{S}^g(u_p,v_p,u,v)}{\tilde{K}(u_p,v_p,u,v)} * \tilde{V}(u_p,v_p,u,v)$$

Equation similar to the classical relation between the gridded dirty image, gridded dirty beam, and beam-apodized sky brightness distribution

Problems:

- if we continue working with $P^g(u_p,v_p,u,v)$ it is not possible to correct for the griding convolution
- otherwise a deconvolution (4D) is already needed to obtain $P(u_p,v_p,u,v)$

Griding and sampling in 2D (u,v)

$$S(l_p, m_p, u, v) \longrightarrow S(u, v)$$
$$K(l_p, m_p, u, v) \longrightarrow K(u, v)$$

Limiting cell size

Gridding in (l_p, m_p) by observational procedure

$$V^g(l_p, m_p, u, v) \equiv K(u, v) * [V(l_p, m_p, u, v) \cdot S(u, v)]$$
$$S^g(u, v) \equiv K(u, v) * S(u, v)$$

FT(V^g) ⟶

$$P^g(u_p, v_p, u, v) = K(u, v) * [P(u_p, v_p, u, v) \cdot S(u, v)]$$

Griding correction and final imaging and deconvolution

$$\tilde{I}^g_{uv}(u_p, v_p) = \frac{P^g(u_p, v_p, u, v)}{\tilde{B}(u_p, v_p)}$$

$$FT_{uv}[\frac{P^g(u_p, v_p, u, v)}{\tilde{B}(u_p, v_p)}] = \frac{1}{\tilde{B}(u_p, v_p)} FT_{uv}[K(u, v) * \{P(u_p, v_p, u, v) \cdot S(u, v)\}]$$

$$\frac{I^g}{\tilde{K}} = \frac{1}{\tilde{B}}[\tilde{P} * \tilde{S}] = \frac{1}{\tilde{B}}[\tilde{P} * \frac{\tilde{S}^g}{\tilde{K}}]$$

Map size and scanning velocity

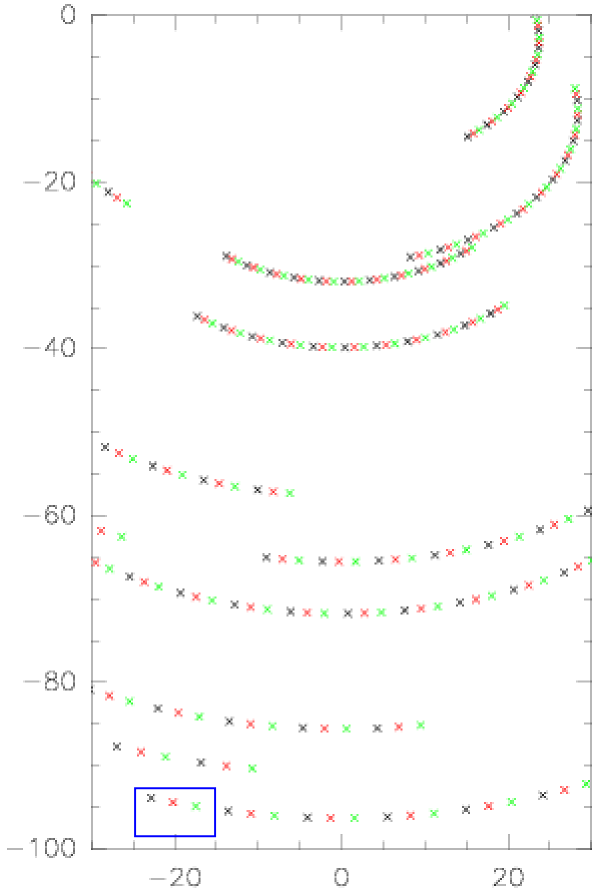

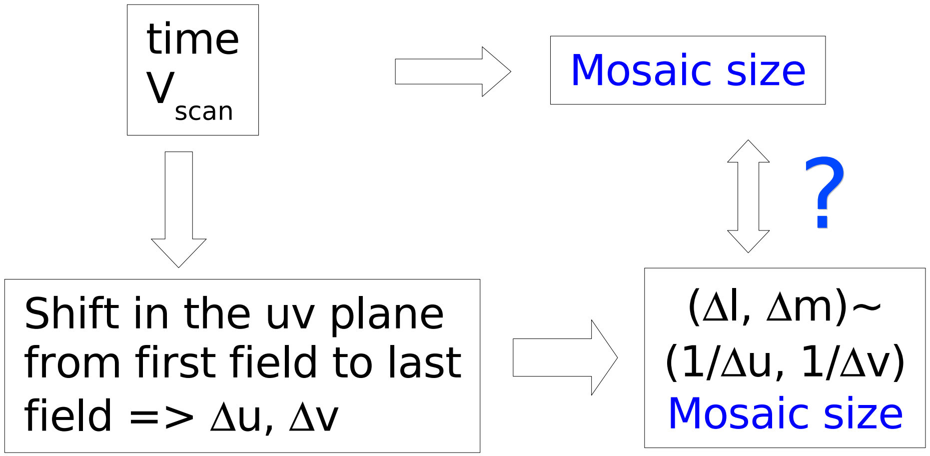

v_{scan} arcsec/sec	time min	map linear size arcmin
0.5	18	1.9
1	14	2.4
5	8.8	4
10	7	5
20	5.4	6.5
40	4.4	8
60	3.8	9.1

PdBI
δ=30º

Dumping time

PdBI
δ=30º

min t_{dump}=1 sec ⇨
⇨ max v_{scan}=10''/sec

v_{scan} arcsec/sec	time min	map linear size arcmin
0.5	18	1.9
1	14	2.4
5	8.8	4
10	7	5
20	5.4	6.5
40	4.4	8
60	3.8	9.1

Summary

- We have now an On-the-fly (OTF) observations simulator to develop OTF-specific imaging techniques.

- We have done feasibility studies of OTF-specific imaging algorithms.
  - The general case is far from trivial...
  - A workaround is to impose some constrains on the observation procedures (Cartesian grids, mosaic size)

PS: In addition, we have done analytical and numerical calculations of the error transfer in the pseudovisibilities computations to optimize the addition of short-spacing data to wide-field interferometric observations

What next ?

- Publications of reports:
  - Short spacings addition: pseudovisibilities weights
  - Feasibility studies of OTF-specific imaging algorithms
- Implementation of the *restricted* algorithm
- Exploration of the limits of the algorithm using the OTF simulator as input data

Weights and global uv plane

$$\tilde{I}^g_{uv}(u_p, v_p) = \frac{P^g(u_p, v_p, u, v)}{\tilde{B}(u_p, v_p)}$$

σ^2

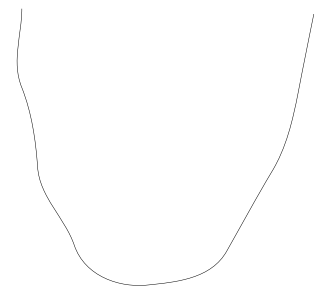

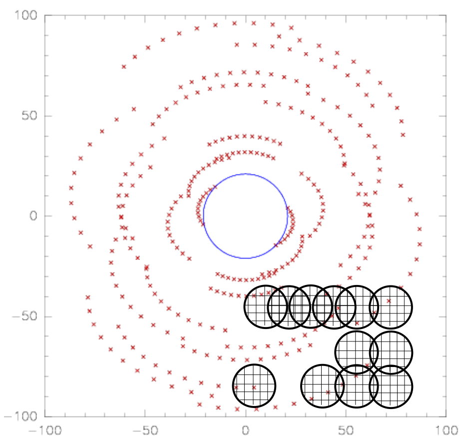

$$\tilde{I}^{gT}(u_i, v_j) = \sum_{mn} \frac{\omega_{u_m,v_n} I^g_{u_m,v_n}(u_{p_k}, v_{p_l})}{\omega^2_{u_m,v_n}} \; ; \quad \forall\, u_m \text{ with } \; u_m + u_{p_k} = u_i$$

On the griding in the uv plane

We can be sure that the uv points corresponding to the different fields are not shifted to a distance larger than the cell size ...

... but this does not mean that they will lie exactly in the same cell, they can be in contiguous cells ...

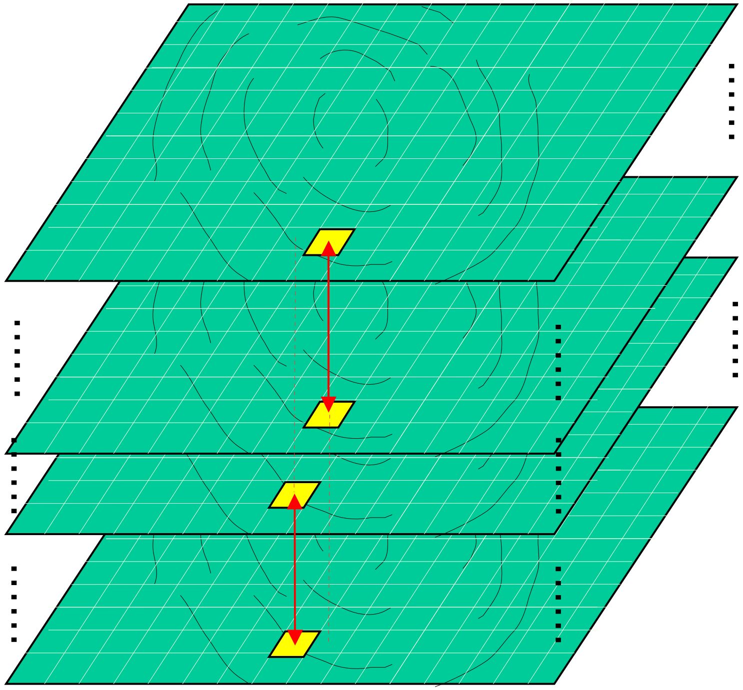

... and to be close to the theory we should have a measurement of the visibility at a the same (u,v) point for all the mosaic fields

Dumping time & effective beam

$$V(u,l_p) = \int_{t_0}^{t_0+t_{dump}} dt/t_{dump} \int dx B(l - l_p(t))\, I(l)\, e^{-i2\pi ul}$$

$$B_{eff}(l) = \int_{t_0}^{t_0+t_{dump}} dt B(l - l_p(t))/t_{dump}$$

$$B_{eff}(l) = B(l) * \Pi(l/(2v_{scan}t_{dump}))$$

$$\tilde{B}_{eff}(u) = \tilde{B}(u) \cdot \mathrm{sinc}(u \cdot (2v_{scan}t_{dump}))$$

$(V_{scan}\, t_{dump})$ < 1/3 FWHM of the primary beam